

On vertical turbulent buoyant jets

R. M. C. SO and H. AKSOY

Mechanical and Aerospace Engineering, Arizona State University, Tempe, AZ 85287-6106,
U.S.A.

(Received 23 October 1992 and in final form 16 February 1993)

Abstract—Plane and round buoyant jets in a quiescent ambient have three distinctive regions; an initial variable-density, non-buoyant region, a transition region and a final plume region. Decay laws in the first and third regions can be derived from dimensional similarity considerations. However, the decay relations in the transition region are usually determined empirically. This paper presents an approach whereby decay laws valid for all three regions are derived for plane and round buoyant jets. The analysis is carried out by assuming self-preservation of the mean field in each of the regions and Gaussian error distributions for the mean properties. With this formulation, the eddy diffusivities for momentum and temperature (or mass fraction) are determined by solving the turbulent mean flow equations subject to appropriate boundary conditions and are found to vary along and across the jet. An auxiliary equation is derived by requiring the eddy viscosity to correctly approach its corresponding limiting value for an incompressible free plane or round jet. The auxiliary equation thus derived is physically related to jet entrainment. Growth rate and decay laws are deduced and they correctly predict their dependence on the jet density ratio in the first region and the densimetric Froude number in the third region. Calculations of decays of centerline properties in these two regions correlate well with plane and round jet measurements. On the other hand, decays of centerline properties in the transition region are dependent on both the jet density ratio and the densimetric Froude number and are in good agreement with plane and round jet data.

INTRODUCTION

TURBULENT jets in a quiescent ambient can be classified according to the relative importance of two parameters. One is the initial momentum flux, M , and the other is the initial specific buoyancy flux, B . The jet is a steady plume when M is small compared to B , while it is a pure jet when B is negligible compared to M . It is a buoyant jet when the two parameters are of comparable importance. However, even in a vertical turbulent buoyant jet, different flow regimes can be identified downstream of the jet exit depending on the relative influence of M and B (Fig. 1). In general, three distinct regions exist [1]. An initial variable-density, non-buoyant region, where B is not important, occurs near the jet exit. The flow in this region is essentially the same as that found in a variable-density, non-buoyant jet and can be similarly analysed. This is followed by a transition region, where M and B play equally important roles in determining the characteristics of the jet. The third region of a buoyant jet is a plume. In this region, the flow is far from the source; therefore, the effects of M are negligible and B becomes the only important parameter. Consequently, the plume region can be analysed by methods used to study steady plumes. This means that the flow in the first and third regions can be analysed by dimensional similarity considerations. However, in the transition region, such an analysis is not presently available; thus, growth rate and decay laws are not well defined and calculations of these properties have to rely on empirical correlations.

Since the flow in the first region only depends on M and the jet density ratio, σ_1 , it can be analysed in a manner similar to that of variable-density, non-buoyant jets. Besides the assumptions that the flow is fully-developed and remains axisymmetric or planar throughout the region of interest, the analysis usually invokes the assumption that the eddy viscosity is constant across the jet and that the turbulent Prandtl or Schmidt number is constant [2, 3]. Under these assumptions, Gaussian distributions are obtained for the mean velocity and mean scalar; however, the linear jet growth rate and hyperbolic centerline decay of velocity and scalar can be recovered correctly only when the centerline eddy viscosity is considered constant [3]. Since then, a more general analysis has been presented [4]. The analysis postulates separate Gaussian error distributions for the mean velocity and mean scalar and relaxes the constant turbulent Prandtl or Schmidt number assumption. Distributions for the eddy momentum and eddy scalar diffusivities can then be obtained by solving the turbulent mean flow equations. Physically realistic boundary conditions, such as finiteness at the jet centerline and at the jet edge and the correct approach to their incompressible values, are specified [5]. The analysis gives rise to rather general expressions for the diffusivities and they are functions of both the streamwise and radial (or normal) coordinates. Thus derived, the eddy viscosity can be used to deduce an auxiliary equation which is solved together with the integral equations to yield linear jet growth rate and hyperbolic centerline decays for the mean properties. The results are in very good agreement with measurements, including those

NOMENCLATURE

a	constant, $c + c_1$	V	mean radial velocity
b	constant, $a + c$	x	axial coordinate measured from jet exit
B	initial specific buoyancy flux, $gQ(\rho_\infty - \rho_j)/\rho_\infty$	X	dimensionless x coordinate, x/D .
B_1	constant defined for incompressible plane jets, $\delta'_u/4c$	Greek symbols	
B_2	constant defined for incompressible round jets, $4c^2D/Re_t\delta_j$	α_t	eddy thermal conductivity
c	constant defined in equation (9a)	β	coefficient of thermal expansion for water
c_1	constant defined in equation (9b)	γ_0	centerline buoyancy flux per unit volume, $g(\rho_\infty - \rho_0)$
D	jet nozzle diameter	$\bar{\gamma}_0$	normalized γ_0 , $\gamma_0/g(\rho_\infty - \rho_j)$
A_1, A_2, A_3, A_4	coefficients introduced in equation (16)	δ_u	jet velocity half-width defined in Fig. 1
E	entrainment function	δ_t	jet temperature half-width defined in Fig. 1
F	entrainment coefficient	δ_j	jet velocity half-width evaluated at jet exit
Fr_j	densimetric Froude number, $[\rho_j U_j^2/gD(\rho_\infty - \rho_j)]^{1/2}$	$\bar{\delta}_u$	dimensionless δ_u , δ_u/δ_j
Fr_L	local Froude number, $[\rho_0 U_0^2/gD(\rho_\infty - \rho_0)]^{1/2}$	η	dimensionless r coordinate, r/δ_u
g	gravitational constant	Θ	mean excess temperature, $T - T_\infty$
H	diffusivity function defined in equation (15b)	Θ_0	centerline excess temperature
H_1	diffusivity function defined in equation (22b)	Θ_j	centerline excess temperature evaluated at jet exit
i	index used to denote non-buoyant ($i = 0$) and buoyant ($i = 1$) jets	$\bar{\Theta}_0$	normalized centerline excess temperature, Θ_0/T_∞
l_M	characteristic lengthscale, $M^{3/4}/B^{1/2}$	θ	fluctuating temperature
m	specific momentum flux, $\int_{\text{jet}} U^2 2\pi r dr$	μ_t	turbulent viscosity
M	initial specific momentum flux, QU_j	ρ	mean density
Pr_t	turbulent Prandtl number	ρ_0	centerline mean density deficit, $\rho_\infty - \bar{\rho}_0$
q	volume flux, $\int_{\text{jet}} U 2\pi r dr$	ρ_j	jet fluid density
Q	initial volume flux, $\pi D^2 U_j/4$	ρ_∞	fluid density of external stream
r	radial (or normal) coordinate measured from symmetry axis	$\bar{\rho}_0$	centerline mean density, $\rho_\infty - \bar{\rho}_0$
Re_t	turbulent Reynolds number, $\lim_{\eta \rightarrow 0} [(\delta_u(0)U_0(0)/\nu_t(0,\eta)) \cdot (H(0,\eta)/\eta^2)]$	$\bar{\rho}_0$	normalized centerline mean density deficit, $\bar{\rho}_0/(\rho_\infty - \rho_j)$
T	mean temperature	σ_1	jet density ratio, ρ_j/ρ_∞ .
T_∞	temperature of the external stream	Subscripts	
u	fluctuating axial velocity	j	jet exit condition
U	mean axial velocity	0	jet centerline condition
U_j	jet velocity	r	reference condition
U_0	velocity at the jet centerline	∞	external stream condition.
\bar{U}_0	normalized jet centerline velocity, U_0/U_j	Superscripts	
v	fluctuating radial velocity	'	differentiation with respect to x
		j	index used to denote plane ($j = 0$) and round ($j = 1$) jet.

obtained from heated jets and binary gas jets of helium and carbon dioxide [4].

The approach taken to solve the plume problem is slightly different from that used to tackle variable-density, non-buoyant jets. Besides the usual jet flow assumptions, the analysis also invokes the Boussinesq approximation, i.e. the variation of density throughout the flow field is small compared to the density level. Under this additional assumption, the flow is influenced by B alone and is independent of σ_1 . In the

past, researchers avoid the difficulties of turbulence modeling and attempt to solve the plume problem through the use of integral methods [6–12]. Based on experimental evidence [13], Gaussian distributions are assumed for the mean velocity and mean scalar. Therefore, the governing equations can be integrated across the jet cross-section to yield ordinary differential equations for the centerline properties. An auxiliary equation is required to close the set and this is usually obtained from entrainment consideration

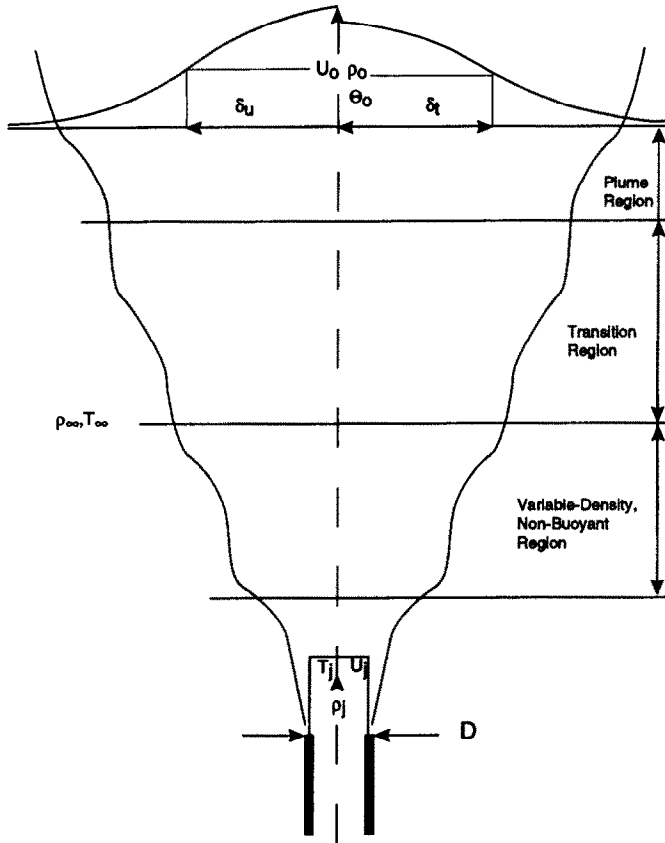


FIG. 1. The three different regions of a buoyant jet.

modeled after the proposal of Morton *et al.* [6]. This involves postulating the ambient fluid entrainment rate and essentially trades the empiricism of turbulence modeling to that of modeling jet entrainment and, therefore, jet spread. Presumably, jet entrainment is not only a function of M but also depends on B and σ_1 . In other words, different entrainment rate equations have to be proposed for plumes with different densimetric Froude numbers, Fr_j and σ_1 [14].

These different approaches yield fairly good results when they are applied to treat variable-density, non-buoyant jets and plumes separately. However, they are not appropriate for analysing the entire region of a buoyant jet. Some attempts have been made to remedy this shortcoming [6, 15, 16]. Since the integral relations obtained from the governing equations are valid for all three regions of the buoyant jet, dimensional similarity analysis can be applied to treat the entire region if a suitable entrainment rate or fourth equation can be found. Such proposals have been put forward by Morton *et al.* [6], Fox [15] and Davis *et al.* [16] for plane and round jets. However, all three proposals involve different empirical constants even though they are formulated for buoyant jets with the same parameters. Furthermore, they cannot be easily generalized to jets with different initial conditions. For example, all three proposals for entrainment rate

assume that σ_1 is not important. According to the analysis of variable-density, non-buoyant jets by So and Liu [4], this assumption is not quite valid. Their results show that heavier-fluid jets spread faster and decay slower than lighter-fluid jets and the difference is substantial. For example, it is found that a carbon dioxide jet spreads faster by 42% and its centerline velocity decays slower by 29% at a normalized downstream location of $X = 10(\delta_j/D)(Re_j/4c^2)$ compared to a helium jet with the same jet exit velocity. In view of this, any entrainment rate equation that ignores the effect of σ_1 is limited and cannot be easily generalized to treat buoyant jets with different Fr_j and σ_1 .

Of course, this difficulty can be avoided by taking a completely different approach to tackle the buoyant jet problem. This involves solving the governing equations by finite-difference techniques and assuming appropriate turbulence models for the turbulent momentum and scalar fluxes [17, 18]. Closure of the turbulence equations can be achieved by different levels of modeling. The commonly used model requires the solution of two extra equations that govern the transport of the turbulent kinetic energy and its dissipation rate. In addition, gradient transport and constant turbulent Prandtl or Schmidt number assumptions are invoked so that the turbulent momentum and scalar fluxes can be related to a com-

mon eddy viscosity and their respective mean velocity and mean scalar gradient. The eddy viscosity is determined from the turbulent kinetic energy and its dissipation rate. In the process of modeling the turbulent fluxes, no less than five model constants are introduced and their values are determined from experiments on incompressible free jets, flat-plate boundary layers and homogeneous decaying turbulence. Unfortunately, no single set of constants is equally applicable to both plane and round jets. If the jet spread of both types of jets is to be calculated correctly, some constants have to take on different values for round jets [17, 18]. The difficulty is related to jet entrainment and it seems that presently there is no satisfactory way to resolve this issue for turbulent plane and round buoyant jets; the explanation of Pope [19] for incompressible plane and round jets notwithstanding. Basically, as pointed out by Pope [19], the difference lies in vortex stretching which affects entrainment, but is absent in plane jets. Recently, Cho and Chung [20] derived an intermittency equation taking into account the effect of entrainment and incorporated it into the $k-\epsilon$ turbulence model. Their model calculations of two-dimensional and axisymmetric free shear flows showed marked improvements over conventional models. Consequently, their results lend support to the argument that it is important to account for entrainment effects properly in the calculations of free shear layers, be it incompressible or buoyant flows.

The present objective is to make an attempt to resolve the issue of entrainment rate for vertical turbulent buoyant jets. Instead of trying to propose an entrainment function valid for both types of jets, the present study attempts to derive separate entrainment functions for the plane and round jet, respectively. An integral approach is used to accomplish this objective. Separate Gaussian error distributions are assumed for the mean velocity and mean scalar and the conservation equations are integrated to give a general distribution for the eddy viscosity. The eddy viscosity is required to satisfy certain physical boundary conditions at the centerline and at the edge of the jet. If the eddy viscosity is further required to approach its incompressible plane and round jet value correctly, a separate auxiliary equation, similar to an entrainment rate equation, is obtained for plane and round jets, respectively. This equation and the integral conservation equations can be solved to yield growth rate and decay laws for the entire region of the plane and round buoyant jet.

THE GOVERNING EQUATIONS

Plane and round vertical turbulent buoyant jets in a quiescent ambient are considered (Fig. 1). The flow is assumed to be steady and fully-developed in the mean field at a relatively short distance downstream of the jet exit. The assumption of mean field self-preservation does not imply self-preservation of the turbulence field. Indeed, as later analysis shows, the

turbulent momentum and heat fluxes do vary along the jet. Their variations are fully described by the derived turbulent diffusivities which are functions of both the stream coordinate and a dimensionless radial (or normal) coordinate. Evidence in support of mean field self-preservation can be gleaned from the recent binary gas jet measurements of So *et al.* [21]. According to ref. [21], fully-developed characteristics of the mean velocity and density are evident as early as $9D$ downstream of the jet exit. Therefore, similarity analysis of the mean field can be applied to all three regions of the buoyant jet. Furthermore, the flow Reynolds number is considered to be very large so that molecular diffusion is negligible and all fluid properties except density are taken to be constant. Under these assumptions, the mean flow equations for the temperature and mass fraction are identical. Therefore, solutions of binary gas buoyant jets are identical to heated buoyant jets. In view of this, only heated jets are considered below. Once the solution to the temperature field is obtained, the corresponding solution to the mass fraction scalar also is available. Invoking thin shear layer approximations, the governing equations for the turbulent buoyant jet can be written as:

$$\frac{\partial}{\partial x}(\rho U r^i) + \frac{\partial}{\partial r}(\rho V r^i) = 0, \quad (1)$$

$$\begin{aligned} \frac{\partial}{\partial x}(\rho U^2 r^i) + \frac{\partial}{\partial r}(\rho U V r^i) \\ = -ig(\rho - \rho_\infty) r^i + \frac{\partial}{\partial r}(-r^i \rho \bar{w}), \end{aligned} \quad (2)$$

$$\frac{\partial}{\partial x}(\rho U \Theta r^i) + \frac{\partial}{\partial r}(\rho V \Theta r^i) = \frac{\partial}{\partial r}(-r^i \rho \bar{v} \theta) - \rho U r^i \frac{dT_x}{dx}, \quad (3)$$

$$\rho T = \rho_\infty T_\infty. \quad (4)$$

In writing down (3) and (4), the pressure is assumed constant everywhere consistent with the thin shear layer approximations. The index i is used to denote the presence of buoyancy effects; therefore, $i = 0$ represents variable-density, non-buoyant jets while $i = 1$ denotes buoyant jets. Boundary conditions for (1)–(4) can be stated as:

$$U(x, \infty) = \Theta(x, \infty) = 0, \quad \rho(x, \infty) = \rho_\infty, \quad (5a)$$

$$U(x, 0) = U_0(x), \quad V(x, 0) = 0, \quad \Theta = \Theta_0(x)$$

$$\rho(x, 0) = \rho_\infty - \rho_0(x) = \bar{\rho}_0(x), \quad (5b)$$

where the centerline values are to be determined.

If the symmetry conditions at the jet centerline and vanishing turbulent fluxes in the ambient are used to simplify the integrals of (1)–(3), the following results are obtained:

$$\frac{d}{dx} \int_0^\infty \rho U r^i dr = -(\rho V r^i)_\infty = E, \quad (6)$$

$$\frac{d}{dx} \int_0^\infty \rho U^2 r^i dr = ig \int_0^\infty (\rho_\infty - \rho) r^i dr, \quad (7)$$

$$\frac{d}{dx} \int_0^\infty \rho U \Theta r' dr = - \frac{dT_\infty}{dx} \int_0^\infty \rho U r' dr. \quad (8)$$

These equations can be reduced into ordinary differential equations if the mean velocity and mean density distributions are expressed in terms of a radial (or normal) coordinate made dimensionless by an appropriately defined jet width $\delta_u(x)$. The four unknowns in the problem are δ_u and the centerline properties U_0 , ρ_0 and Θ_0 . Only three equations are available and these are (4), (7) and (8). Even though (6) is an entrainment equation, it is not an appropriate fourth equation because E is not known. Since (4), (7) and (8) are uniformly valid for the entire jet region, the solutions obtained are equally applicable to the three regions of the buoyant jet if and only if the fourth equation to be derived is equally valid for the three regions.

THE MEAN FLOW

The approach used by So and co-workers [4, 5, 22, 23] to derive the fourth equation is to assume distributions for U and ρ and then use the mean flow equations to solve for the behavior of the momentum and heat fluxes across the jet. If the assumption of gradient transport is invoked, the behavior of the eddy momentum and heat diffusivities can be determined from the corresponding turbulent flux behavior. Physically realizable boundary conditions are imposed on the eddy diffusivities and they are then used to deduce equations that describe jet entrainment and the variation of eddy momentum to heat diffusivity. When this approach is used to treat incompressible heated free jets [5], general expressions for μ_t and α_t are obtained. So and Hwang [5] show that the only distributions for mean velocity and temperature that will lead to physically realistic expressions for μ_t and α_t are Gaussian error functions. Extensions of this approach to treat isothermal binary gas jets [4], incompressible heated jets in a co-flowing stream [22] and variable-density, non-buoyant jets in a uniform stream [23] also have been carried out. Again, the physically valid distributions for mean velocity and temperature (or mass fraction) are Gaussian error functions. In all these cases, the approach leads to an auxiliary equation that gives rise to a general entrainment function. The predicted growth rate and decay laws are in good agreement with measurements.

If the same approach is used to treat buoyant jets, physically realistic distributions have to be assumed for the mean velocity and temperature (or mass fraction). The measurements of Rouse *et al.* [13] indicate that these functions can be suitably correlated by Gaussian distributions. Subsequent experiments on plane [24–26] and round jets [21, 27–32] lend further credence to the findings of Rouse *et al.* [13]. For example, when the Gaussian distribution $\exp[-G(r/x)^2]$ is used to correlate an appropriately defined dimensionless mean velocity, the exponent G is found to

vary for different jets. On the other hand, if the Gaussian error distribution $\exp[-c(r/\delta_u)^2]$ is used to correlate all velocity data, c remains constant for all jets [25]. This is true provided that δ_u is taken to be the jet half-width which is defined as the radial (or normal) location where the mean velocity is equal to half its value at the jet centerline (Fig. 1). With this definition for δ_u , c is determined to be $\ln 2$. Similar distributions can be found for the mean temperature and mass fraction. If δ_u is again used to normalized r for these distributions, the exponent c_1 is found to remain constant; however, its value cannot be determined analytically. Once U and ρ are known, the distributions of V and Θ can be determined from (1) and (4). The turbulent fluxes can be obtained by integrating (2) and (3). However, these functions are not fully determined because they depend on jet growth and the decays of centerline properties. Therefore, a complete solution is available if and only if the growth rate and the decays of centerline properties also are determined.

In view of the above arguments, Gaussian error functions given by

$$U = U_0(x) \exp[-c\eta^2], \quad (9a)$$

$$\rho_x - \rho = \rho_0(x) \exp[-c_1\eta^2], \quad (9b)$$

$$\rho\Theta = T_\infty \rho_0(x) \exp[-c_1\eta^2], \quad (9c)$$

are assumed for the mean flow field in the present approach to analyse plane and round buoyant jets. It can be easily shown that (9c) is a direct consequence of (9b) and (4). The exponent c is, by definition, equal to $\ln 2$; however, c_1 is not known and its value has to be determined from experimental measurements. Based on the study of So and Liu [4], c_1 is found to range in value from 0.34 to 0.56 for σ_1 that varies from 0.14 to 1.52. Therefore, a ten fold increase in σ_1 only results in a 50% increase in c_1 . According to the definitions of δ_t and δ_u , c_1/c is equal to $(\delta_u/\delta_t)^2$. Therefore, c_1 also can be determined from the relative spread rate of the velocity and temperature layer. The normalized radial (or normal) coordinate is taken to be $\eta = r/\delta_u$. With these substitutions and the further assumption that the ambient temperature is constant, (4) evaluated at the centerline and (6)–(8) can be written as

$$\rho_\infty [U_0 \delta_u^{j+1}]' \int_0^\infty \exp[-c\eta^2] \eta^j d\eta = E, \quad (10)$$

$$\begin{aligned} &\rho_\infty [U_0^2 \delta_u^{j+1}]' \int_0^\infty \exp[-2c\eta^2] \eta^j d\eta \\ &- [\rho_0 U_0^2 \delta_u^{j+1}]' \int_0^\infty \exp[-b\eta^2] \eta^j d\eta \\ &= i \rho_0 g \delta_u^{j+1} \int_0^\infty \exp[-c_1\eta^2] \eta^j d\eta, \quad (11) \end{aligned}$$

$$[\rho_0 U_0 \delta_u^{j+1}]' = 0, \quad (12)$$

$$\tilde{\rho}_0 \Theta_0 = T_\infty (\rho_\infty - \tilde{\rho}_0). \quad (13)$$

These equations can be solved to give δ_u , U_0 , ρ_0 and Θ_0 if E is known. Alternatively, an auxiliary equation can be used to determine jet growth and centerline property decays. In the following, a method is described whereby an auxiliary equation is derived from (1) and (2) with the help of (9a) and (9b) and physically realistic boundary conditions for the turbulent momentum and heat fluxes. The auxiliary equation thus derived can be shown to be related to jet entrainment. Therefore, an entrainment coefficient can be determined and compared to empirical entrainment coefficients proposed by other researchers [6, 15, 16]. For the sake of clarity, the auxiliary equations for the round and plane jets are derived separately in the next two sections. Once this is accomplished, the corresponding entrainment functions are deduced. Thus derived, the entrainment functions are uniformly valid for the entire region of the jet.

AN AUXILIARY EQUATION FOR ROUND JETS

For round jets, $j = 1$ and the integrals of the various exponentials can be made exact and evaluated analytically. Therefore, with the help of (1), (9a) and (9b), (2) can be evaluated to give

$$\begin{aligned} \rho \bar{u} \bar{w} = & \left[\rho_x (2\delta'_u U_0^2 + \delta_u U_0 U'_0) \right. \\ & - \frac{c}{a} \{2\rho_0 \delta'_u U_0^2 + \delta_u U_0 (\rho_0 U_0)'\} \left. \right] \frac{\exp(-c\eta^2)}{2c\eta} \\ & - \left[\frac{\rho_x \delta'_u U_0^2}{2c} \right] \frac{\exp(-2c\eta^2)}{\eta} \\ & - \left[\frac{ig\delta_u \rho_0}{2c_1} \right] \frac{\exp(-c_1\eta^2)}{\eta} \\ & + \left[\frac{c}{a} \{2\rho_0 \delta'_u U_0^2 + \delta_u U_0 (\rho_0 U_0)'\} \right. \\ & \left. - \rho_0 \delta_u U_0 U'_0 \right] \frac{\exp(-b\eta^2)}{2b\eta}. \end{aligned} \tag{14}$$

It can be seen that $\rho \bar{u} \bar{w}$ goes to zero as η increases indefinitely. On the other hand, the behavior of $\rho \bar{u} \bar{w}$ at the jet centerline depends on the behavior of the centerline properties. In order to analyse this behavior, gradient transport is assumed for $\rho \bar{u} \bar{w}$ and the eddy viscosity μ_t is defined in terms of a function $H(x, \eta)$ so that

$$-\rho \bar{u} \bar{w} = \mu_t \frac{\partial U}{\partial r} \quad \text{and} \quad \mu_t = \left[\frac{\tilde{\rho}_0 \delta_u U_0}{Re_t} \right] \frac{H(x, \eta)}{\eta^2}. \tag{15a,b}$$

The rationale for defining μ_t by (15b) is to insure that it will take on the limiting incompressible free jet value correctly as ρ approaches ρ_x . According to So and Hwang [5], (H/η^2) is only a function of η for incompressible free jets. Therefore, for buoyant jets, the

general form for (H/η^2) should be functions of both x and η . Substitution of (15) into (14) results in the following expression for H :

$$H = A_1 + A_2 \exp(-c\eta^2) + A_3 \exp\{-c(c_1 - c)\eta^2\} + A_4 \exp(-a\eta^2), \tag{16}$$

$$A_1 = \frac{Re_t}{4c^2 \tilde{\rho}_0 U_0^2} \left[\rho_x (2\delta'_u U_0^2 + \delta_u U_0 U'_0) - \frac{c}{a} \{2\rho_0 \delta'_u U_0^2 + \delta_u U_0 (\rho_0 U_0)'\} \right], \tag{17a}$$

$$A_2 = - \left[\frac{Re_t}{4c^2} \right] \frac{\rho_x \delta'_u}{\tilde{\rho}_0}, \tag{17b}$$

$$A_3 = - \left[\frac{Re_t}{4cc_1} \right] \frac{ig\rho_0 \delta_u}{\tilde{\rho}_0 U_0^2}, \tag{17c}$$

$$A_4 = \frac{Re_t}{4bc\tilde{\rho}_0 U_0^2} \left[\frac{c}{a} \{2\rho_0 U_0^2 \delta'_u + \delta_u U_0 (\rho_0 U_0)'\} - \delta_u \rho_0 U_0 U'_0 \right], \tag{17d}$$

where the coefficients A_1, A_2, A_3 and A_4 are functions of x and their behavior will be known once the variations of the centerline properties are defined. At the jet centerline, the mean velocity gradient vanishes. In order for $\rho \bar{u} \bar{w}$ to vanish there, μ_t has to be finite. The condition for this to be true is given by: $A_1 + A_2 + A_3 + A_4 = 0$. Since the integrals from left to right in (11) can be evaluated and their values are $(1/4c)$, $(1/2b)$ and $(1/2c_1)$, respectively, the value of $(A_1 + A_2 + A_3 + A_4)$ can be determined with the help of (11) and (12) and is identically zero. Consequently, the physical requirements that μ_t is finite and $\rho \bar{u} \bar{w}$ vanishes at the jet centerline are satisfied.

The next step is to impose the condition that μ_t has to approach its value for incompressible free jet correctly. This way, the free jet is a special solution of the more general solution presented here. For the case of an incompressible free jet, $i = 0$, $\rho_0 = 0$, $\tilde{\rho}_0 = \rho_x$ and $(\delta'_u U_0^2)' = 0$. Therefore, $A_3 = A_4 = 0$ and $A_1 = -A_2 = (Re_t/4c^2)\delta'_u$. According to So and Hwang [5], there is no loss of generality if A_1 is chosen to be 1. This means that all arbitrary constants in the formulation are accounted for by Re_t . With this choice for A_1 and A_2 , (H/η^2) is only dependent on η . Thus defined, the limiting value of (H/η^2) as η goes to zero is c . If the argument is made that μ_t approaches its incompressible value correctly, then the behavior of (H/η^2) at the jet centerline should be the same for all jets and the limiting value of (H/η^2) as η goes to zero also should be c . This condition gives rise to $-A_2c - A_3(c_1 - c) - aA_4 = c$. The auxiliary equation derived from this condition is given by

$$\delta'_u + \frac{a}{2c} \left[\frac{(\delta''_u U_0^2)'}{\delta_u U_0^2} \right] - \frac{2c}{c_1} \left[\frac{ig\rho_0 \delta_u}{\rho_x U_0^2} \right] = \frac{4c^2}{Re_t} \left(\frac{\tilde{\rho}_0}{\rho_x} \right). \tag{18}$$

Equation (18) can be interpreted as an equation for the jet spread. The effects of buoyancy and the variations of centerline properties on jet growth are clearly indicated. Furthermore, (18) reduces exactly to the expression given above for an incompressible free jet.

An expression for the entrainment function E can now be derived. Since the integral in (10) is equal to $(1/2c)$, (10)–(12) and (18) can be used to determine E . Omitting all the tedious algebra, the result is

$$E = \frac{\rho_\infty (\delta_u^2 U_0)'}{2c} = 2\delta_u \rho_\infty U_0 \left[\frac{2c^2}{b Re_t} \left(\frac{\tilde{\rho}_0}{\rho_\infty} \right) - \frac{c_1}{4bc} \left(\frac{\delta_u U_0'}{U_0} \right) + \frac{c}{bc_1} \left(\frac{i}{Fr_L^2} \right) \left(\frac{\delta_u \rho_0^2}{D \rho_\infty \tilde{\rho}_0} \right) \right]. \quad (19)$$

In writing down this expression, the perimeter of the jet is taken to be $2\delta_u$. According to Morton *et al.* [6], E can also be written as $E = (2\delta_u)' \rho_\infty U_0 F$ for both plane and round jets, where F is the entrainment coefficient. Therefore, F can be deduced from (19) and the result is

$$F = \left[\frac{2c^2}{b Re_t} \left(\frac{\tilde{\rho}_0}{\rho_\infty} \right) - \frac{c_1}{4bc} \left(\frac{\delta_u U_0'}{U_0} \right) + \frac{c}{bc_1} \left(\frac{i}{Fr_L^2} \right) \left(\frac{\delta_u \rho_0^2}{D \rho_\infty \tilde{\rho}_0} \right) \right]. \quad (20)$$

Several empirical expressions also have been proposed for F . These can be written in the common form:

$$F = 0.057 + \frac{a_2}{Fr_L^n}, \quad (21)$$

where a_2 is a constant and differs in value from one proposal to the next, $n = 1$ is specified by Morton *et al.* [6] and Fox [15] and $n = 0.3$ is chosen by Davis *et al.* [16]. The present entrainment coefficient not only shows dependence on Fr_L , but also on the decays of centerline properties. Therefore, it is more realistic and its derivation is not as ad hoc as that of (21).

An expression for the eddy thermal conductivity can be similarly derived. This is obtained by integrating (3) with the help of (9). If gradient transport is again assumed for the turbulent heat flux and, consistent with (15b), a similar functional relation is invoked for α_i , then $\rho \bar{v}\bar{\theta}$ and α_i can be represented by

$$-\rho \bar{v}\bar{\theta} = \alpha_i \frac{\partial \Theta}{\partial r} \quad \text{and} \\ \alpha_i = \left[\frac{\tilde{\rho}_0 \delta_u U_0}{Re_t} \right] \left(\frac{\rho}{\rho_\infty} \right) \frac{H_1(x, \eta)}{\eta^2}. \quad (22a, b)$$

The present form suggested for α_i is necessary because the physical boundary conditions, such as vanishing turbulent heat flux at the jet centerline and in the ambient fluid, the finiteness of α_i at the jet center and the correct approach of the turbulent Prandtl number, Pr_t , at the centerline to its incompressible heated jet value, have to be satisfied. With the turbulent heat flux thus defined, substitution of (9) and (22) into (3)

gives rise to the following expression for H_1 ,

$$H_1 = \frac{Re_t \rho_\infty (\delta_u^2 U_0)'}{2c_1 \tilde{\rho}_0 \delta_u U_0} \left[\frac{1 - \exp(-c\eta^2)}{2c} \right]. \quad (23)$$

It can be easily shown that H_1 and hence $\rho \bar{v}\bar{\theta}$ and α_i satisfy the physical conditions specified above and that Pr_t is deduced to be $Pr_t = (\rho_\infty H / \rho H_1)$. In the limit of η goes to zero, Pr_t approaches c_1/c ; a value identical to that obtained for incompressible heated free jets [5, 19]. Since $c_1/c = (\delta_u/\delta_t)^2$, Pr_t also can be interpreted as a measure of the relative spread of the velocity layer to that of the thermal layer. The present approach determines the variation of the spread ratio rather than assuming it to be constant.

AN AUXILIARY EQUATION FOR PLANE JETS

Once the methodology is established, it is fairly simple to derive the corresponding equations for a plane jet ($j = 0$). One exception to note is that, when (1)–(3) are integrated with the help of (9), the integrals appearing in the equations will no longer give rise to exponential functions as in the case of the round jet. Instead, they will appear as error functions. Consequently, fairly cumbersome expressions are obtained for the integrated form of (1)–(3) and μ_i and α_i cannot be easily cast into forms similar to (15b) and (22b) with relatively simple expressions for H and H_1 . The integral in (10) is evaluated to give $\sqrt{(\pi/4c)}$, while those in (11) from left to right are: $\sqrt{(\pi/8c)}$, $\sqrt{(\pi/4b)}$ and $\sqrt{(\pi/4c_1)}$, respectively. In the following, expressions for μ_i and α_i are presented and an auxiliary equation is derived by requiring μ_i to approach its incompressible plane jet value in the limit of η goes to zero and $i = 0$. Omitting all algebra and, noting that for plane jets, (12) reduces to $(\delta_u \rho_0 U_0)' = 0$, the dimensionless μ_i is given by

$$\frac{\mu_i}{\delta_u \tilde{\rho}_0 U_0} = -\frac{1}{2} \sqrt{\left(\frac{\pi}{2c} \right) \frac{\rho_\infty (\delta_u U_0^2)'}{\tilde{\rho}_0 U_0^2}} \left[\frac{\exp(c\eta^2)}{2c\eta} \right] \\ \times \operatorname{erf}(\sqrt{(2c)\eta}) + \frac{1}{2} \sqrt{\left(\frac{\pi}{c} \right) \frac{\rho_\infty U_0 (\delta_u U_0)'}{2c\tilde{\rho}_0 U_0^2}} \frac{\operatorname{erf}(\eta\sqrt{c})}{\eta} \\ + \frac{1}{2} \sqrt{\left(\frac{\pi}{b} \right) \frac{\rho_0 \delta_u (U_0^2)'}{2\tilde{\rho}_0 U_0^2}} \left[\frac{\exp(c\eta^2)}{2c\eta} \right] \operatorname{erf}(\eta\sqrt{b}) \\ + \frac{1}{2} \sqrt{\left(\frac{\pi}{c_1} \right) \frac{ig\rho_0 \delta_u}{2c\tilde{\rho}_0 U_0^2}} \left[\frac{\exp(c\eta^2)}{\eta} \right] \operatorname{erf}(\eta\sqrt{c_1}). \quad (24)$$

In the limit of η goes to zero and $i = 0$, (24) can be shown to reduce to $\delta_u'/4c$ which is the value for an incompressible jet. Since the growth rate of an incompressible plane jet is linear, $\delta_u'/4c$ is a constant. Denoting this constant by B_1 , an auxiliary equation can be obtained by requiring that, in the limit of η goes to zero, (24) approaches B_1 . The result is

$$B_1 = -\frac{\delta_u U_0 U_0'}{2c U_0^2} + \frac{ig\rho_0 \delta_u}{2c\tilde{\rho}_0 U_0^2}. \quad (25)$$

An entrainment function can now be derived from (10), (11) and (25). From (10), E is determined to be

$$E = \rho_x U_0 F = \rho_x (\delta_u U_0)' \sqrt{\left(\frac{\pi}{4c}\right)}, \quad (26)$$

while (11) can be re-arranged to yield

$$\begin{aligned} -\frac{\delta_u U_0 U_0'}{2cU_0^2} \left[\rho_x - \rho_0 \sqrt{\left(\frac{2c}{b}\right)} \right] \\ = \frac{\rho_x U_0 (\delta_u U_0)'}{2cU_0^2} - \frac{ig\rho_0 \delta_u}{2cU_0^2} \sqrt{\left(\frac{2c}{c_1}\right)}. \end{aligned} \quad (27)$$

Combining (25)–(27), the entrainment coefficient for plane jets can be written as

$$\begin{aligned} F = \frac{\sqrt{(\pi c)}}{B_1} \left(1 - \frac{\rho_0}{\rho_x} \sqrt{\left(\frac{2c}{b}\right)} \right) + Fr_L^2 \left(D\rho_x \bar{\rho}_0 \right) \\ \times \left[\sqrt{\left(\frac{\pi}{2c_1}\right)} + \frac{1 - (\rho_0/\rho_x) \sqrt{(2c/b)}}{1 - (\rho_0/\rho_x)} \sqrt{\left(\frac{\pi}{4c}\right)} \right]. \end{aligned} \quad (28)$$

Again, it can be seen that F depends on Fr_L and the variations of centerline properties. It is quite different from (20) and (21). This means that a single proposal, such as (21), for both plane and round jets would not be appropriate. Furthermore, (28) is not based on ad hoc assumptions for jet entrainment. Therefore, it would be more realistic compared to (21).

An expression for α_i can be similarly derived. Without going into details, the result is

$$\begin{aligned} \frac{\alpha_i}{\delta_u \bar{\rho}_0 U_0 (\rho/\rho_x)} = \frac{\delta_u'}{2c_1} [1 - \exp(-c_1 \eta^2)] \\ \times \exp[-(c - c_1) \eta^2] + \frac{(\delta_u U_0)'}{4c_1 U_0} \left(\frac{\rho_x}{\bar{\rho}_0} \right) \\ \times \sqrt{\left(\frac{\pi}{c}\right)} \frac{\exp(c_1 \eta^2)}{\eta} \operatorname{erf}(\eta \sqrt{c}), \end{aligned} \quad (29)$$

where the reference quantities chosen to make α_i dimensionless are the same as those adopted in the round jet case. It can be shown that (29) satisfies the requirements that the heat flux vanishes at the jet centerline as well as at infinity. Furthermore, Pr_i evaluated in the limit of η goes to zero for the case of an incompressible plane jet is again given by $Pr_i = c_1/c$. Therefore, just as in the case of round jets, the classical results for incompressible plane jets are recovered correctly.

JET GROWTH AND DECAYS OF CENTERLINE PROPERTIES

The four equations that govern jet growth and centerline decays are given by (11)–(13) and (18) for round jets and (11)–(13) and (27) for plane jets. In terms of normalized variables, the four non-dimensional equations for round jets become

$$\bar{\Theta}_0 = \frac{(1 - \sigma_1) \bar{\rho}_0}{1 - (1 - \sigma_1) \bar{\rho}_0}, \quad (30)$$

$$(\delta_u^{j+1} \bar{\rho}_0 \bar{U}_0)' = 0, \quad (31)$$

$$(\bar{\delta}_u^2 \bar{U}_0^2)' - \frac{2c}{b} (1 - \sigma_1) (\bar{\delta}_u^2 \bar{\rho}_0 \bar{U}_0^2)' - \frac{2c}{c_1} \left(\frac{i\sigma_1}{Fr_j^2} \right) \bar{\rho}_0 \bar{\delta}_u^2 = 0, \quad (32)$$

$$\bar{\delta}_u' + \frac{a}{2c} \frac{(\bar{\delta}_u^2 \bar{U}_0^2)'}{\bar{\delta}_u \bar{U}_0^2} - \frac{2c}{c_1} \left(\frac{i\sigma_1}{Fr_j^2} \right) \frac{\bar{\rho}_0 \bar{\delta}_u}{\bar{U}_0^2} = B_2 [1 - (1 - \sigma_1) \bar{\rho}_0]. \quad (33)$$

As for plane jets, the four non-dimensional equations are given by (30), (31) with $j = 0$ and the following two equations that are deduced from (12) and (27). These are

$$\begin{aligned} (\bar{\delta}_u \bar{U}_0^2)' - (1 - \sigma_1) \sqrt{\left(\frac{2c}{b}\right)} (\bar{\delta}_u \bar{\rho}_0 \bar{U}_0^2) \bar{U}_0' \\ - \sqrt{\left(\frac{2c}{c_1}\right)} \frac{i\sigma_1}{Fr_j^2} \bar{\delta}_u \bar{\rho}_0 = 0, \end{aligned} \quad (34)$$

$$\begin{aligned} [1 - (1 - \sigma_1) \bar{\rho}_0] (\bar{\delta}_u \bar{U}_0) \bar{U}_0' + \frac{i\sigma_1}{Fr_j^2} \bar{\delta}_u \bar{\rho}_0 \\ + 2cB_1 [1 - (1 - \sigma_1) \bar{\rho}_0] \bar{U}_0^2 = 0. \end{aligned} \quad (35)$$

Thus normalized, the equations are parametric in σ_1 and Fr_j and there are two free constants in each set of equations. The constants are c_1 , B_1 and B_2 . Since c_1 has already been determined by So and Liu [4], only B_1 and B_2 need to be evaluated. These constants are related to the spread of incompressible plane and round jets, therefore, they can be determined from these limiting flow cases.

When variable-density, non-buoyant jets are considered, $i = 0$ and the resultant equations are parametric in σ_1 only. These equations are identical to those derived by So and Liu [4]. They found that the jet growth rate is linear and the centerline decays of mean velocity and density are hyperbolic. Therefore, in the first region of a buoyant jet, the jet growth and centerline decays are known. In the transition region, both σ_1 and Fr_j are of equal importance. Therefore, the complete equations given above have to be solved. Further downstream, in the plume region, it can be easily determined from dimensional similarity considerations that \bar{U}_0 would decay like $X^{-1/3}$ and $\bar{\rho}_0$ would behave like $X^{-5/3}$ for round jets and that \bar{U}_0 would be constant and $\bar{\rho}_0$ would go like X^{-1} for plane jets. It can be shown that this asymptotic behavior is given by the solutions of the above equations with $i = 1$ and $\sigma_1 = 1$. Thus, the jet characteristics are parametric only in Fr_j . In view of this, the strategy for solving the buoyant jet problem is to start the calculation using the variable-density, non-buoyant jet equations. The initial conditions for these equations are $\bar{\delta}_0 = 1$, $\bar{U}_0 = 1$, $\bar{\rho}_0 = 1$ and $\bar{\Theta}_0 = (1 - \sigma_1)/\sigma_1$ specified at the jet exit. The calculation is continued

until the asymptotic behavior is obtained. This solution is used to determine the virtual origin of the buoyant jet and the various quantities thus determined are used as initial conditions for the solution of the buoyant jet equations. Their solutions give the growth rate and centerline decays for both the transition and plume regions, because far enough downstream, the solutions of (30)–(35) would approach asymptotically the plume behavior.

RESULTS AND DISCUSSION

Parametric calculations are carried out to show the dependence of the decays of centerline properties on σ_1 and Fr_j . Since the equations for plane and round jets are first order, non-linear ordinary differential equations, they can be solved by a number of standard numerical techniques. A standard Runge–Kutta algorithm is used in the present study. The calculations are performed by first solving the variable-density, non-buoyant jet equations using the jet exit conditions as initial conditions. Since the growth rate is linear and the decay laws are hyperbolic for these non-buoyant jets, the parametric calculations can be carried out by choosing the constants B_1 and B_2 to be 1, hence the products of \bar{U}_0 and X and $\bar{\rho}_0$ and X follow to be 1. In view of this choice of constants, the growth rates of the plane and round jets are not shown. Only the centerline decays of \bar{U}_0 and $\bar{\rho}_0$ are presented. The centerline decay of $\bar{\Theta}_0$ follows directly from (30), and, hence, is also not shown. With the solution of the initial region known, the buoyant jet equations are solved using the non-buoyant jet solution as initial conditions. In addition to specifying σ_1 , Fr_j also has to be given. Since the start of the transition region depends on Fr_j , a trial and error technique has to be used to determine this location. Once this is determined, the solution of the equations is carried out until the asymptotic plume behavior is reached. Combining these solutions will yield a composite solution to the governing equations.

Only sample results for plane and round jets are shown. In the case of round jets, the results to be presented are for $\sigma_1 = 0.4$ and three different values of Fr_j ranging from 3.162 to 316.2. This is equivalent to specifying Fr_j^2 from 10 to 10^5 . On the other hand, the results to be presented for plane jets are for $Fr_j = 22.36$ and three different values of σ_1 ranging from 0.1 to 0.95. This way, the effects of σ_1 and Fr_j on centerline decays in the transition region can be clearly illustrated. The results for the round jet are given in the set of Figs. 2–5, while those for the plane jet are shown in the set of Figs. 6–9. In the first two figures of each set, the decay curves in the variable-density, non-buoyant region and the transition region are shown in the form of \bar{U}_0 vs X and $\bar{\gamma}_0$ vs X . It should be pointed out that presenting the density behavior in the form of a normalized buoyancy flux is consistent with the practices of other researchers [1]; however, the non-dimensional buoyancy flux as defined is ident-

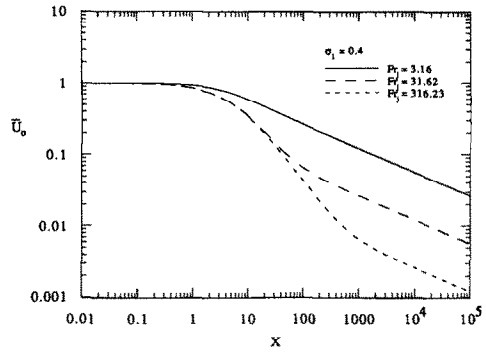


FIG. 2. Decay of \bar{U}_0 for three different values of Fr_j for a round jet.

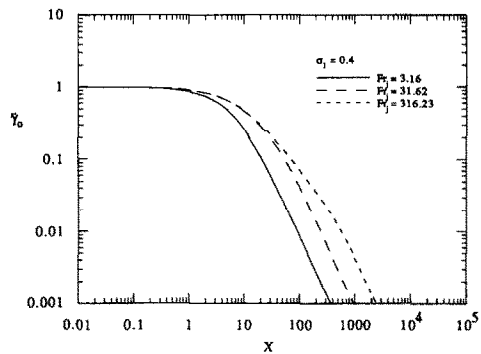


FIG. 3. Decay of $\bar{\gamma}_0$ for three different values of Fr_j for a round jet.

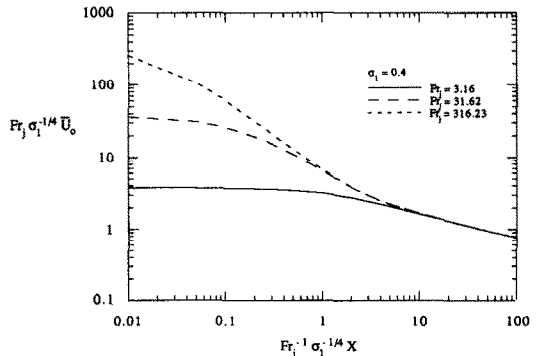


FIG. 4. A plot of $Fr_j \sigma_1^{-1/4} \bar{U}_0$ vs $Fr_j^{-1} \sigma_1^{-1/4} X$ for three different values of Fr_j for a round jet.

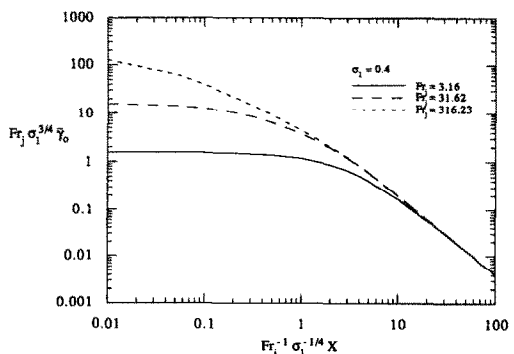


FIG. 5. A plot of $Fr_j \sigma_1^{3/4} \bar{\gamma}_0$ vs $Fr_j^{-1} \sigma_1^{-1/4} X$ for three different values of Fr_j for a round jet.

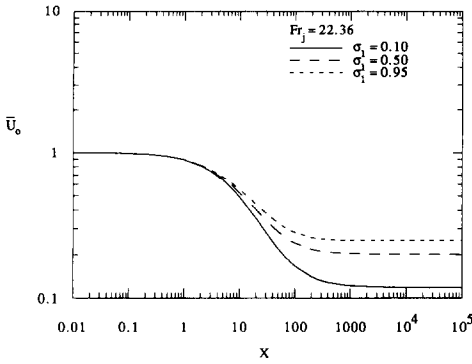


FIG. 6. Decay of \bar{U}_0 for three different values of σ_1 for a plane jet.

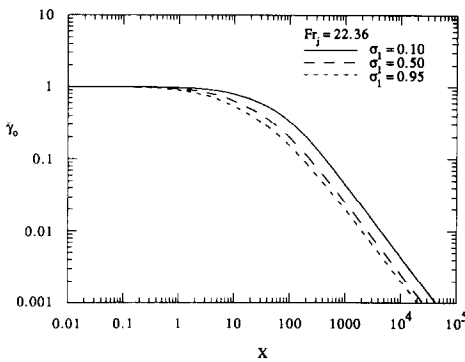


FIG. 7. Decay of $\bar{\gamma}_0$ for three different values of σ_1 for a plane jet.

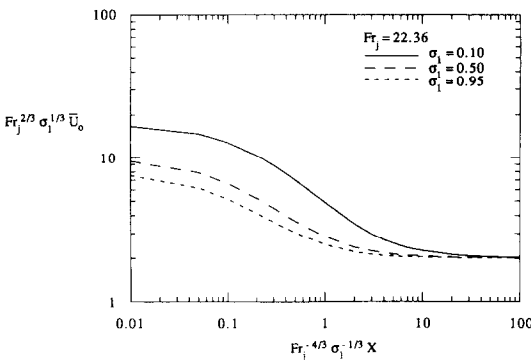


FIG. 8. A plot of $Fr_j^{2/3} \sigma_1^{1/3} \bar{U}_0$ vs $Fr_j^{-4/3} \sigma_1^{-1/3} X$ for three different values of σ_1 for a plane jet.

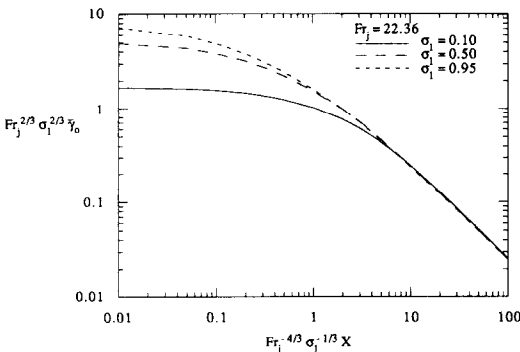


FIG. 9. A plot of $Fr_j^{2/3} \sigma_1^{2/3} \bar{\gamma}_0$ vs $Fr_j^{-4/3} \sigma_1^{-1/3} X$ for three different values of σ_1 for a plane jet.

ical to $\bar{\rho}_0$. The last two figures in each set show the decays in the transition and plume regions and the variables are normalized by both σ_1 and Fr_j in the manner suggested by Chen and Rodi [1]. Therefore, $Fr_j \sigma_1^{-1/4} \bar{U}_0$ is plotted vs $Fr_j^{-1} \sigma_1^{-1/4} X$ and $Fr_j \sigma_1^{-3/4} \bar{\gamma}_0$ is plotted vs $Fr_j^{-1} \sigma_1^{-1/4} X$ in Figs. 4 and 5, respectively. On the other hand, $Fr_j^{2/3} \sigma_1^{1/3} \bar{U}_0$ is plotted vs $Fr_j^{-4/3} \sigma_1^{-1/3} X$ in Fig. 8 and $Fr_j^{2/3} \sigma_1^{2/3} \bar{\gamma}_0$ is plotted vs $Fr_j^{-4/3} \sigma_1^{-1/3} X$ in Fig. 9.

The effect of Fr_j on centerline decays in the transition region of a round jet is clearly illustrated in Figs. 2–5. Note that as Fr_j increases, the length of the initial region for \bar{U}_0 decreases (Fig. 2) while the corresponding length for $\bar{\gamma}_0$ increases (Fig. 3). Initially, the decay of \bar{U}_0 is slower for lower values of Fr_j while the opposite is true for $\bar{\gamma}_0$. However, further downstream, the decay curves for all Fr_j calculated are essentially parallel for \bar{U}_0 and $\bar{\gamma}_0$. This means that the decay rates become the same for all Fr_j calculated. The final plume region is clearly shown in Figs. 4 and 5. Plotted in these dimensionless variables, the decay behavior is essentially independent of Fr_j in the plume region, just as the experimental data suggest [1]. Finally, it should be pointed out that the length of the transition region is very much affected by Fr_j . It decreases as Fr_j increases.

The effect of σ_1 on centerline decays in the transition region of a plane jet is presented in Figs. 6–9. It can be seen that the decay rate for \bar{U}_0 increases (Fig. 6) while that for $\bar{\gamma}_0$ decreases (Fig. 7) as σ_1 decreases. Just as in the round jet case, the decay curves become parallel further downstream. However, the separation between different curves is not as large as in the case of varying Fr_j while keeping σ_1 constant. The length of the initial region also depends on σ_1 . It increases as σ_1 decreases (Fig. 7). Plotting the results in terms of the dimensionless variables suggested by Chen and Rodi [1] again show that decay in the plume region is essentially independent of Fr_j (Figs. 8 and 9). Furthermore, the length of the transition region is also affected by σ_1 . Together, these two sets of results demonstrate that if σ_1 and Fr_j do not differ significantly from one experiment to another, the variations noted in the measured decays may not be very large. Consequently, they could be incorrectly attributed as scatter in the measurements [1].

Comparisons with experimental measurements can now be carried out. In all these calculations, the constants B_1 and B_2 are determined by matching the level of \bar{U}_0 decay with data in the initial region. As for c_1 , it is obtained from the values quoted in ref. [4]. Since most of the measurements to be compared give a σ_1 not too different from 1, $c_1 = 0.533$ is quoted by So and Liu [4]. This value is equivalent to specifying a $Pr_t = 0.74$ for incompressible heated jets. The plane jet calculations are compared with data collected by Harris [24] and Kotsovinos and List [25], while the round jet calculations are validated against the measurements of Ogino *et al.* [30], Papanicolaou and List [31] and Peterson and Bayazitoglu [32]. Most

experiments did not report measurements covering all three regions. The exception is the recent and very careful round jet measurements of Papanicolaou and List [31]; therefore, this set of data can be used to truly assess the correctness of the present analysis. All calculations are carried out by specifying the exact values of σ_1 and Fr_j used in the experiments and in the manner described above. The final values of the constants c_1 , B_1 and B_2 used in the calculations are: $c_1 = 0.533$ and $B_1 = 0.04$ for plane jets; $c_1 = 0.533$ and $B_2 = 0.18$ for round jets. As for the values of σ_1 and Fr_j , they are listed in the respective plots shown in Figs. 10–15. After the results are obtained, they are prepared in the appropriate forms for comparison with measurements.

With the exception of the experiments by Peterson and Bayazitoglu [32], which were conducted in air, the other experiments were carried out in water. Since the equation of state for water is different from that for a perfect gas, there is a need to demonstrate the validity of the present approach when the fluid is water. In a limited temperature range and to the lowest order, the equation of state for water can be written as

$$\frac{1}{\rho} = \frac{(1 - \beta T_r)}{\rho_r} + \frac{\beta}{\rho_r} T, \quad (36)$$

where β is taken to be constant in the temperature range considered. This equation is identical in form to the equation of state for the mixing of binary gases, which is given by [4, 23]

$$\frac{1}{\rho} = \frac{1}{\rho_\infty} - \left(\frac{1}{\rho_\infty} - \frac{1}{\rho_i} \right) \Theta, \quad (37)$$

where Θ in this case is the mixture mass fraction and ρ is the mixture density. The present approach is equally valid when used to analyse mixing of binary gas jets [4, 23] and the same set of equations (31)–(35) with $Fr_j = 0$ would result. In the binary gas jet case, (30) would be replaced by (37) evaluated at the centerline. Therefore, the present approach can also be used to calculate the experiments of refs. [24, 25, 30, 31]. The equation set (31)–(35) is still applicable and the only equation that is different is (30), which has to be replaced by specializing (36) at the centerline. Since the present comparison is carried out with \bar{U}_0 and $\bar{\gamma}_0$ only, there is no need to solve (30) or (36). In other words, the solutions of (31)–(35) are equally applicable to buoyant jets in water.

The plane jet comparisons of centerline decays of \bar{U}_0 and $\bar{\gamma}_0$ are shown in Figs. 10 and 11, respectively. The calculations are carried out at the experimentally specified values of Fr_j and σ_1 . If these values are explicitly given, the same will be used in the present calculations. On the other hand, if the specific values of Fr_j and σ_1 are not explicitly given, they will be estimated as best as possible from other given properties. The final values used are clearly specified in each figure. Mostly, measurements in the transition

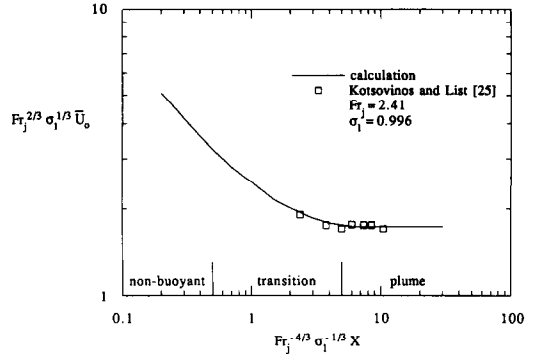


FIG. 10. Comparison of centerline decay of $Fr_j^{2/3} \sigma_1^{1/3} \bar{U}_0$ with measurements for plane jets.

region are selected for comparison with calculations. If possible, data that span at least two regions are chosen. Only one set of velocity comparison is shown in Fig. 10 because of the scarcity of reliable velocity data. However, four sets of density data are compared in Fig. 11 and they span a Fr_j range from 2 to 13. The predictions are in excellent agreement with data over the entire range of the plane buoyant jet. Thus, for the first time, analytical decay laws for the transition region have been derived and are found to yield accurate results.

The comparisons with round jet data are shown in Figs. 12–15. Figures 12 and 13 show the comparisons with the measurements of Ogino *et al.* [30] and Peterson and Bayazitoglu [32] in the range of Fr_j from 5 to 34. Again, the data are selected to span at least two regimes, always covering the transition region. On the other hand, the measurements of Papanicolaou and List [31] covered all three regions of the buoyant jet. Therefore, a comparison with this set of data provides a complete verification of the present theory's ability to predict the jet centerline characteristics in all three regions. Since only normalized centerline volume and momentum fluxes are reported in ref. [31], the calculated results are converted into these quantities for comparison. Furthermore, the axial coordinate is normalized by l_M instead of by the characteristic quantity suggested by Chen and Rodi [1]. Consequently, the comparisons shown in Figs. 14 and 15 are made with these variables. In general, excellent agreement is obtained in all these comparisons; including the decay in the transition region and the asymptotic behavior in the first and third regions. These results further support the validity of the analytically derived decay laws for buoyant round jets.

According to the turbulence modeling study of Launder *et al.* [17], the jet spread and centerline decays of plane and round jets can be predicted correctly provided a modifying function that depends on the decay of centerline velocity is incorporated into the eddy viscosity model for round jets. In other words, the entrainment of external fluid in a round jet would depend to a certain extent on the decay of centerline

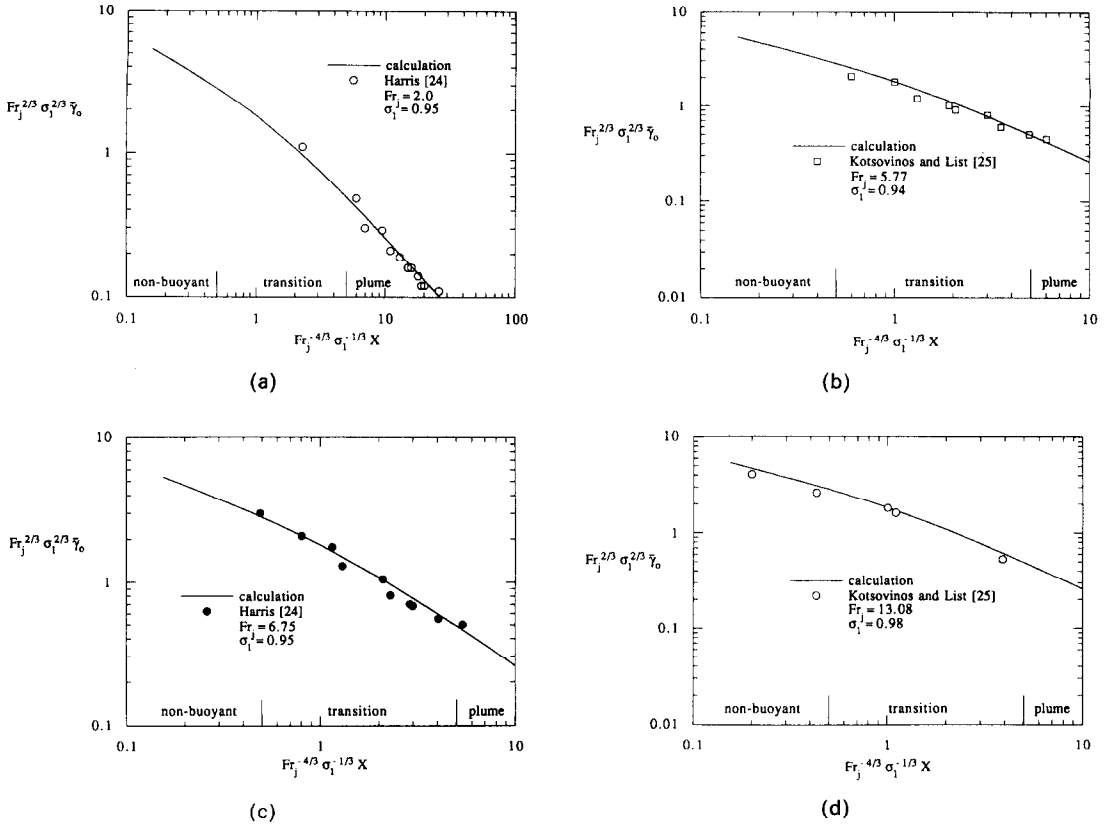


FIG. 11. Comparison of centerline decay of $Fr_j^{2/3} \sigma_1^{2/3} \bar{\gamma}_0$ with measurements for plane jets; (a) $Fr_j = 2.0$; (b) $Fr_j = 5.77$; (c) $Fr_j = 6.75$; (d) $Fr_j = 13.08$.

velocity. The modifying function proposed by Launder *et al.* [17] is empirical and is obtained on an ad hoc basis. This study presents a formal derivation of the separate entrainment function for plane and round buoyant jets and shows that they depend differently on the behavior of the jet centerline properties in addition to their dependence on the local Froude number. It is found that the entrainment coefficient given in (20) for round jets is very much influenced by the decay of centerline velocity. On the other hand,

according to (28), F for plane jets only depends on ρ_0/ρ_∞ and Fr_L and is independent of the decay of U_0 . In view of this, the present investigation essentially verifies the postulate of Launder *et al.* [17]. The validity of the two entrainment functions is demonstrated by comparisons with a wide variety of experimental buoyant jet measurements. Therefore, composite decay laws are available for calculating the decay of centerline properties for the entire region of the plane and round buoyant jet.

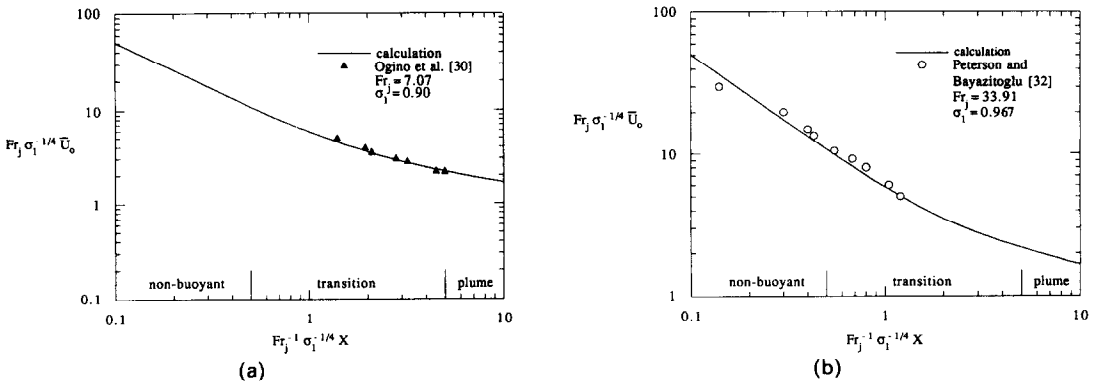
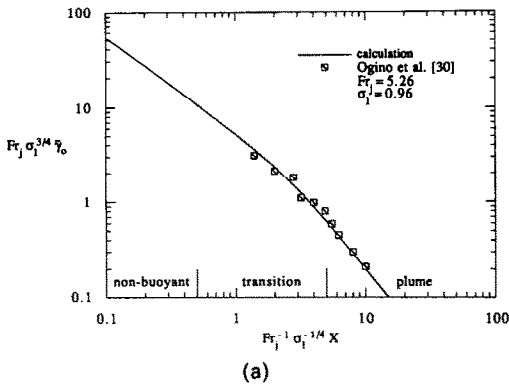
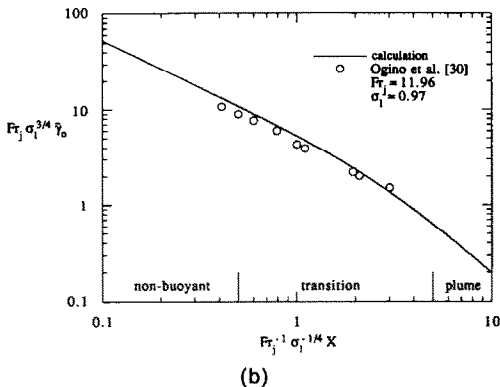


FIG. 12. Comparison of centerline decay of $Fr_j \sigma_1^{-1/4} \bar{U}_0$ with measurements for round jets; (a) $Fr_j = 7.07$; (b) $Fr_j = 33.91$.



(a)



(b)

FIG. 13. Comparison of centerline decay of $Fr_j \sigma_1^{3/4} \bar{\gamma}_0$ with measurements for round jets; (a) $Fr_j = 5.26$; (b) $Fr_j = 11.96$.

Finally, it should be pointed out that the present analysis is not limited to a perfect gas whose equation of state is given by (4) only. As long as the flow is incompressible and the pressure field is constant, the centerline temperature is given by (30) which is derived from (4), while the jet spread and other centerline properties are obtained by solving (31)–(33) or (31), (34) and (35). Since (30) is decoupled from (31)–(35), the solutions of (31)–(35) are independent of the temperature field. In other words, buoyant jets whose equations of state are similar to those given in (4), (36) and (37) can again be analysed using the present approach. Therefore, the present analysis is equally applicable to the study of buoyant jets whose equations of state are linear in terms of density of temperature.

CONCLUSIONS

Three distinct flow regimes exist in a buoyant jet; an initial variable-density, non-buoyant region, a transition region and a final plume region. Dimensional similarity considerations can be used to derive decay laws for the first and third regions only. There are no formal decay laws for the transition region because, in this region, the flow is influenced by both

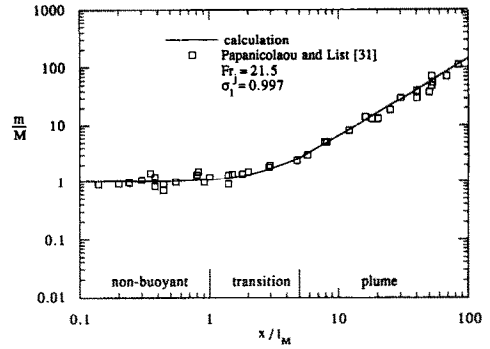


FIG. 14. Comparison of the decay of centerline momentum flux with measurements for round jets.

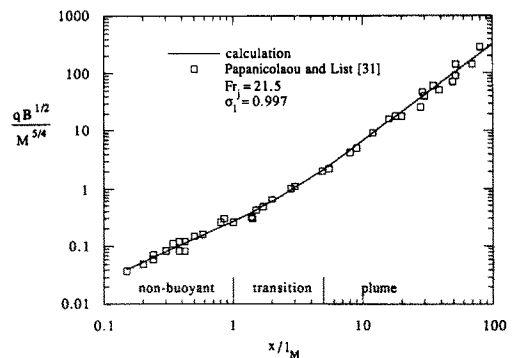


FIG. 15. Comparison of the decay of centerline volume flux with measurements for round jets.

the momentum flux and the buoyancy flux. Different empirical entrainment functions and hence jet growth rates have been put forward; however, they are unsatisfactory because they could not be easily generalized to cover a wide range of jet density ratios and densimetric Froude numbers. The present study proposes a formal approach to derive entrainment functions for plane and round buoyant jets. It is based on the assumption of self-preservation of the turbulent mean flow in each of the three regions of the buoyant jet. Furthermore, Gaussian error distributions are used to describe the mean velocity and mean density and this allows the mean flow equations to be solved for the distributions of turbulent momentum and heat fluxes across the jet. Since these fluxes have to vanish at the jet centerline and at the jet edge, they can be used to determine the distributions of eddy viscosity and eddy thermal conductivity. If the requirement is further made that the eddy viscosity thus determined has to reduce correctly to its incompressible limit, then an expression is obtained for the variations of centerline properties with respect to the non-dimensional axial coordinate. This relation can be reduced to an expression for the entrainment function. Therefore, for the first time, analytically derived entrainment functions are available for plane and round buoyant jets. These analytical expressions are not identical and

are functions of the local Froude number and the decay of centerline properties.

In view of these results, any attempt to propose a single entrainment function for plane and round jets is not appropriate and will not be able to give correct predictions of the characteristics of both plane and round jets. Previously proposed empirical entrainment functions are deficient because they cannot completely account for the effects of centerline decays on the entrainment process. As a result, they cannot be easily generalized for jet flows with widely varying jet density ratios and densimetric Froude numbers. Comparisons of the present calculations with measurements of plane and round buoyant jets over a wide range of densimetric Froude numbers lend credence to the analytically derived entrainment functions. The agreement between predictions and data is excellent in all plane and round buoyant jets examined. The present results further show that the discrepancies noted in the measured decay of centerline properties in the transition region of plane and round buoyant jets are not scatter due to experimental errors. Instead, the discrepancies are the consequence of the dependence of centerline decays on the jet density ratio and the densimetric Froude number.

Acknowledgement—Funding support from Allied Signal Corporation and from Arizona State University in the form of a teaching assistantship to HA is gratefully acknowledged.

REFERENCES

1. C. J. Chen and W. Rodi, *Vertical Turbulent Buoyant Jets—A Review of Experimental Data*. Pergamon Press, New York (1980).
2. P. A. Libby, Theoretical analysis of turbulent mixing of reactive gases with application to supersonic combustion of hydrogen, *ARS J.* **32**, 388–396 (1962).
3. A. Ferri, P. A. Libby and V. Zakkay, Theoretical and experimental investigation of supersonic combustion, *Third Congress, International Council of the Aeronautical Sciences*, pp. 1089–1155. Spartan Books, Baltimore, MD (1964).
4. R. M. C. So and T. M. Liu, On self-preserving, variable-density, turbulent free jets, *Z. Angew. Math. Phys.* **37**, 538–558 (1986).
5. R. M. C. So and B. C. Hwang, On similarity solutions for turbulent and heated round jets, *Z. Angew. Math. Phys.* **37**, 624–631 (1986).
6. B. R. Morton, G. I. Taylor and J. S. Turner, Turbulent gravitational convection from maintained and instantaneous sources, *Proc. R. Soc.* **A234**, 1–23 (1956).
7. B. R. Morton, Forced plumes, *J. Fluid Mech.* **5**, 151–163 (1959).
8. S. L. Lee and H. W. Emmons, A study of natural convection above a line fire, *J. Fluid Mech.* **11**, 353–368 (1961).
9. J. S. Turner, The 'starting plume' in neutral surroundings, *J. Fluid Mech.* **13**, 356–368 (1962).
10. E. J. List and J. Imberger, Concluding discussion of paper 'Turbulent entrainment in buoyant jets and plumes', *J. Hydraul. Div. A.S.C.E.* **101**, 617–620 (1975).
11. E. J. List and J. Imberger, Turbulent entrainment in buoyant jets and plumes, *J. Hydraul. Div. A.S.C.E.* **99**, 1461–1474 (1973).
12. C. S. Yih and F. Wu, Round buoyant laminar and turbulent plumes, *Phys. Fluids* **24**, 794–801 (1981).
13. H. Rouse, C. S. Yih and H. W. Humphreys, Gravitational convection from a boundary source, *Tellus* **4**, 201–210 (1952).
14. B. Gebhart, D. S. Hilder and M. Kelleher, The diffusion of turbulent buoyant jets, *Adv. Heat Transfer* **16**, 1–57 (1984).
15. D. G. Fox, Forced plume in a stratified fluid, *J. Geophys. Res.* **75**, 6818–6835 (1970).
16. L. R. Davis, M. A. Shirazi and D. L. Slegel, Measurement of buoyant jet entrainment from single and multiple sources, *J. Heat Transfer* **100**, 442–447 (1978).
17. B. E. Launder, A. Morse, W. Rodi and D. B. Spalding, Prediction of free shear flows—a comparison of the performance of six turbulence models, NASA SP-321, 361–426 (1972).
18. M. S. Hossain and W. Rodi, A turbulence model for buoyant flows and its application to vertical buoyant jets. In *Turbulent Buoyant Jets and Plumes* (Edited by W. Rodi), pp. 121–178. Pergamon Press, New York (1982).
19. S. B. Pope, An explanation of the turbulent round jet/plane jet anomaly, *AIAA J.* **16**, 279–281 (1978).
20. J. R. Cho and M. K. Chung, A proposal of $k-\epsilon-\gamma$ equation turbulence model, *J. Fluid Mech.* **237**, 301–322 (1992).
21. R. M. C. So, J. Y. Zhu, M. V. Otugen and B. C. Hwang, Some measurements in a binary gas jet, *Exp. Fluids* **9**, 273–284 (1990).
22. R. M. C. So and B. C. Hwang, On incompressible, turbulent, heated round jets in a co-flowing stream, *Aeronaut. J.* **93**, 100–110 (1989).
23. R. M. C. So and H. Aksoy, Gas jet in an arbitrary stream, accepted for publication, *Aeronaut. J.* (in press).
24. P. R. Harris, The densimetric flows caused by the discharge of heated two-dimensional jets beneath a free surface, Ph.D. Thesis, Department of Civil Engineering, University of Bristol, Bristol, England (1967).
25. N. E. Kotsovinos and E. J. List, Turbulent buoyant jets. Part 1. Integral properties, *J. Fluid Mech.* **81**, 25–44 (1977).
26. N. E. Kotsovinos, Plane turbulent buoyant jets. Part 2. Turbulence structure, *J. Fluid Mech.* **81**, 45–62 (1977).
27. C. J. Chen and C. P. Nikitopoulos, On the near field characteristics of axisymmetric turbulent buoyant jets in a uniform environment, *Int. J. Heat Mass Transfer* **22**, 245–255 (1979).
28. B. R. Ramaprian and M. S. Chandrasekhara, Measurements in vertical plane turbulent plumes, *J. Fluids Engng* **111**, 69–77 (1989).
29. W. K. George, R. L. Alpert and F. Tamanini, Turbulence measurements in an axisymmetric buoyant plume, *Int. J. Heat Mass Transfer* **20**, 1145–1154 (1977).
30. F. Ogino, H. Takeuchi, I. Kudo and T. Mizushima, Heated jet discharged vertically into ambients of uniform and linear temperature profiles, *Int. J. Heat Mass Transfer* **23**, 1581–1588 (1980).
31. P. N. Papanicolaou and E. J. List, Investigation of round vertical turbulent buoyant jets, *J. Fluid Mech.* **195**, 341–391 (1988).
32. J. Peterson and Y. Bayazitoglu, Measurements of velocity and turbulence in vertical axisymmetric isothermal and buoyant jets, *J. Heat Transfer* **114**, 135–142 (1992).